Reactivation, trishear modeling, and folded basement in Laramide uplifts: Implications for the origins of intracontinental faults

Alexander P. Bump, Department of Geosciences, University of Arizona, Tucson, Arizona 85721, USA*

ABSTRACT

Laramide uplifts are bounded by reverse faults of enigmatic origin. Two end-member hypotheses have been proposed: (1) they formed during the Laramide orogeny as newly formed contractional features; and (2) they formed as normal faults at some previous time and were reactivated during the Laramide. This paper employs the trishear fault-fold model to test these ideas, based on the premise that, in (1), neoformed faults should propagate from a regional detachment or crustal flaw within the crystalline basement, whereas in (2), reactivated normal faults should begin their Laramide propagation from the base of the Paleozoic cover (i.e., top of basement). Trishear folding takes place entirely ahead of the propagating fault tip, so trishear modeling of fold-fault geometries can be used to evaluate these alternate possibilities. This paper documents 23 uplifts that show a folded basement-cover contact demonstrating that fault propagation began within the basement. Inverse and forward modeling suggest, however, that the faults began propagating only a few kilometers below the basement-cover contact, too shallow for a regional detachment. It is suggested that these faults represent the formation of footwall shortcuts (i.e., lower angle, mechanically easier paths to the surface) to bypass the steep upper sections of reactivated listric faults. This idea unites the two end-member hypotheses, allowing the large-scale map pattern of uplifts to be controlled by reactivated faults at depth while exposing neoformed offshoots of those faults at the surface.

INTRODUCTION

The processes of fault reactivation (Holdsworth et al., 2001) and tectonic inversion (Coward, 1994) of old faults are among the most important issues in continental tectonics. Continental crust, unlike oceanic crust, records the cumulative history of multiple periods of tectonism, and much of continental deformation is focused into large-scale fault networks that are repeatedly reactivated over long time scales. The seismogenic upper crust may be the strongest layer (Jackson, 2002), and hence a stress guide for whole-lithosphere deformation (Axen et al., 1998). To understand a range of seismogenic processes, it is essential to better resolve the interplay between old fault networks and new tectonic stress conditions (Huntoon, 1993; Marshak et al., 2000; Timmons et al., 2001). This paper uses the unique geometries of the Laramide uplifts in the southwestern United States to explore the importance of reactivation versus new fault development in response to Laramide contractional deformation.

The Late Cretaceous–early Tertiary Laramide orogeny has been of particular interest to tectonicists because the horizontal shortening due to plate convergence was expressed within the continental foreland at distances up to twice as far from the plate margin as the more typical and partly contemporaneous Sevier fold-thrust belt (Fig. 1). Style of contractional deformation in the Laramide province is also different from that of the thrust belt, involving a series of fault-bounded, basement-cored uplifts of varying size, orientation, and structural relief. In a few places, such as Rattlesnake Mountain and the Grand Canyon, the uplift-bounding faults are exposed at the surface. In most places, however, they remain blind, either covered by Cenozoic sediments, or expressed at the surface as a monoclinal fault-propagation fold of Paleozoic and Mesozoic strata. Although the geometry and kinematics of some of these faults are relatively well understood, their origin (date of initial rupture) is often difficult to establish. Two end-member hypotheses have been proposed: (1) they formed during the Laramide orogeny (Hamilton, 1988); and (2) they formed at some previous time(s) and were reactivated during the Laramide (Walcott, 1890; Huntoon, 1993; Marshak et al., 2000).

Perhaps the more favored model has been that many, if not most, Laramide faults are reactivated ancient weaknesses, and in a few cases this can be proven directly. For example, Laramide reverse faulting raised Precambrian rift strata along ancient faults in the Uinta Mountains of Utah and the Beltian embayment of Montana. Likewise, Walcott (1890), Huntoon (1993), and Timmons et al. (2001) documented exposures in the Grand Canyon with Precambrian syn-extensional strata present in the hanging wall of Laramide reverse faults but not in the footwall. Similar evidence for reactivation has also been reported for Laramide faults exposed in the Salt River Canyon in central Arizona (Davis et al., 1981) and exhumed fault blocks in southwestern Montana (Schmidt and Garihan, 1983). Detailed studies of fault zone rocks have also yielded clear evidence of reactivation, showing diachronous deformation at different metamorphic grades (Mitra and Frost, 1981).

These examples are exceptions, however. While many Laramide uplifts offer excellent hanging wall exposure, the footwalls and the uplift-bounding faults are often buried beneath significant thicknesses of syn-orogenic and younger sediments (Tweto, 1979; Love and Christiansen, 1985). Many other Laramide faults never broke the surface and are expressed only as monoclinal fault-propagation folds (Tweto, 1979; Hintze, 1980; Love and Christiansen, 1985). Seismic data often do not have the resolution necessary to document stratigraphic evidence for inversion, and

*Present address: BP North American Exploration, 501 Westlake Park Boulevard, Houston, Texas 77079, USA, bumpa1@bp.com.

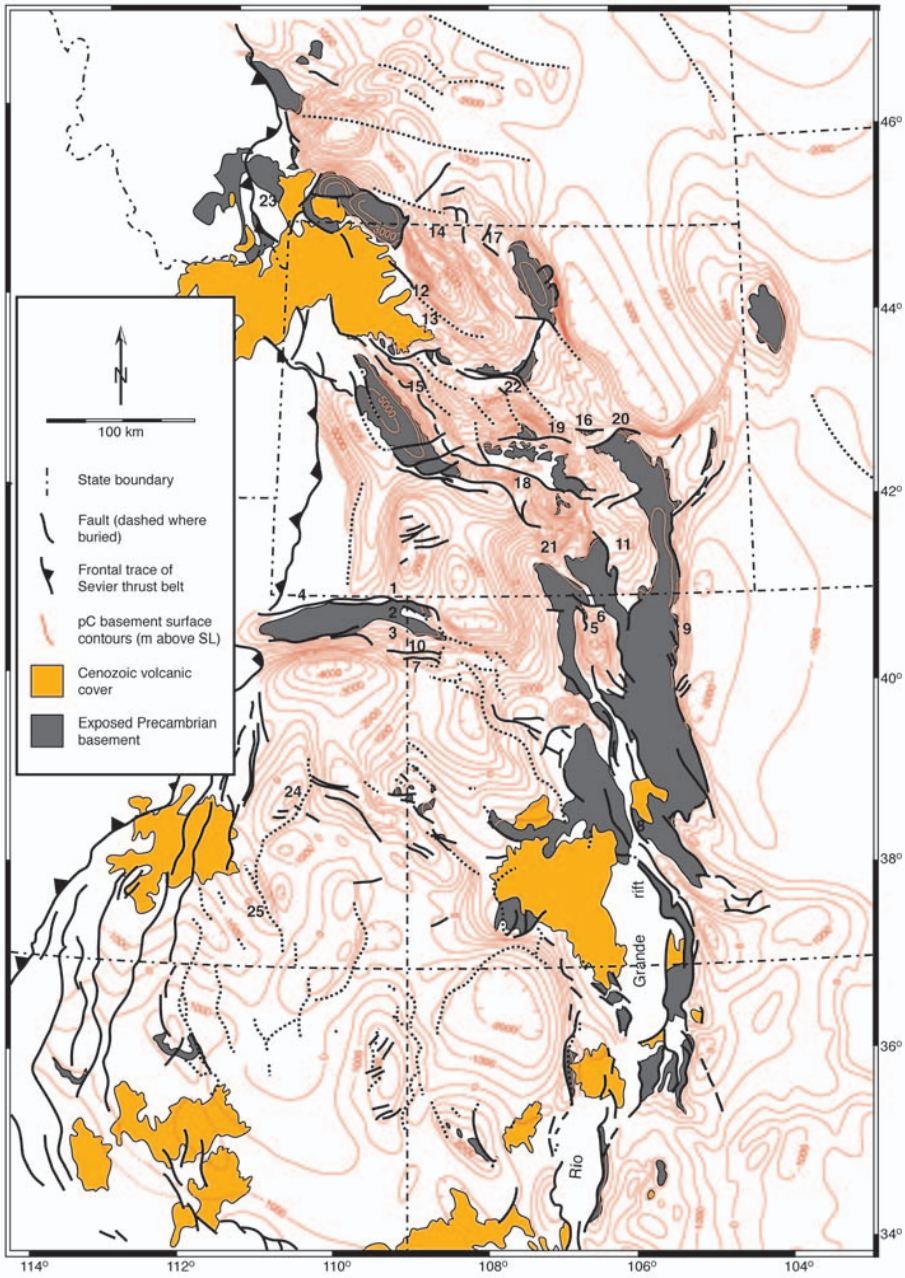

Figure 1. Map of the Laramide orogen (after King, 1969), showing locations of uplifts discussed in the text. Numbers 24 and 25 are the San Rafael Swell and the Circle Cliffs uplifts, respectively. All others are given in Table 1.

boreholes seldom penetrate basement in the footwall, negating the possibility of documenting differences in Precambrian stratigraphy (if present) in the hanging wall and footwall. Thus, for most Laramide faults, the argument for reactivation hinges chiefly on circumstantial evidence. First, Laramide fault strikes show a scatter uncommon in neoformed fault systems such as the extensional faults of the Basin and Range. More specifically, the large-scale map pattern of Laramide faulting is dominated by N-S and NW-SE strikes (Fig. 1) that are similar to those of known Precambrian rifts in the southern Rocky Mountains (Erslev, 1993; Marshak et al., 2000; Timmons et al., 2001). Second, in some cases, Laramide faults parallel nearby Precambrian dikes or shear zones, suggesting that their geometry was governed by associated Precambrian weaknesses (Schmidt and Garihan, 1983). Third, Marshak et al. (2000) pointed out that vergence variations within the Laramide province resemble those of rift provinces, with opposite vergence on either side of the province.

Some authors (Hamilton, 1988; Yin, 1994) have opposed the idea of widespread reactivation, arguing instead that the major uplift-bounding Laramide faults are neoformed features created during the Laramide orogeny. Indeed, most faults show no direct evidence of a pre-Laramide history.

The purpose of this paper is to examine evidence for fault ancestry based on a relatively new criterion: the location of the initial fault tip (Allmendinger and Shaw, 2000; Allmendinger et al., 2003). The initial fault tip location is defined here as the point from which the fault tip began its upward propagation (growth) under Laramide compression. A preexisting fault reactivated in compression could be expected to begin propagating upward from the base of the postorogenic strata (Allmendinger et al., 2003). In the case of the Laramide, that would indicate an initial fault tip depth at the top of the Precambrian, i.e., at the basement-cover contact. Alternatively, a neoformed reverse fault could be expected to do one of two things: either it might propagate upward from a horizontal detachment near the brittle-ductile transition where shear stresses are theoretically highest (Sibson, 1977; Ranalli, 2000), or it might begin with simultaneous up-dip and down-dip propagation from some initial earthquake focus at a flaw or stress concentration in the crust (Allmendinger et al., 2003).

FAULT-PROPAGATION FOLD MODELS

For Laramide faults that began growing in the Late Cretaceous or early Tertiary and are still buried, there is no way to observe the initial tip point directly. However, its location can be inferred through geometric modeling of fold-fault relationships based on structural exposures at the surface and available subsurface information. The key parameter is the propagation to slip (*p/s*) ratio, which describes the distance the fault tip moves (propagates) per unit displacement of the hanging wall. The *p/s* ratio is an inherent feature of all kinematic models of fault-propagation folding, though most treat it only implicitly (Suppe and Medwedeff, 1990; Narr and Suppe, 1994; Mitra and Mount, 1998). The power of the *p/s* ratio lies in its capacity to determine the location of the fault tip prior to fault slip,

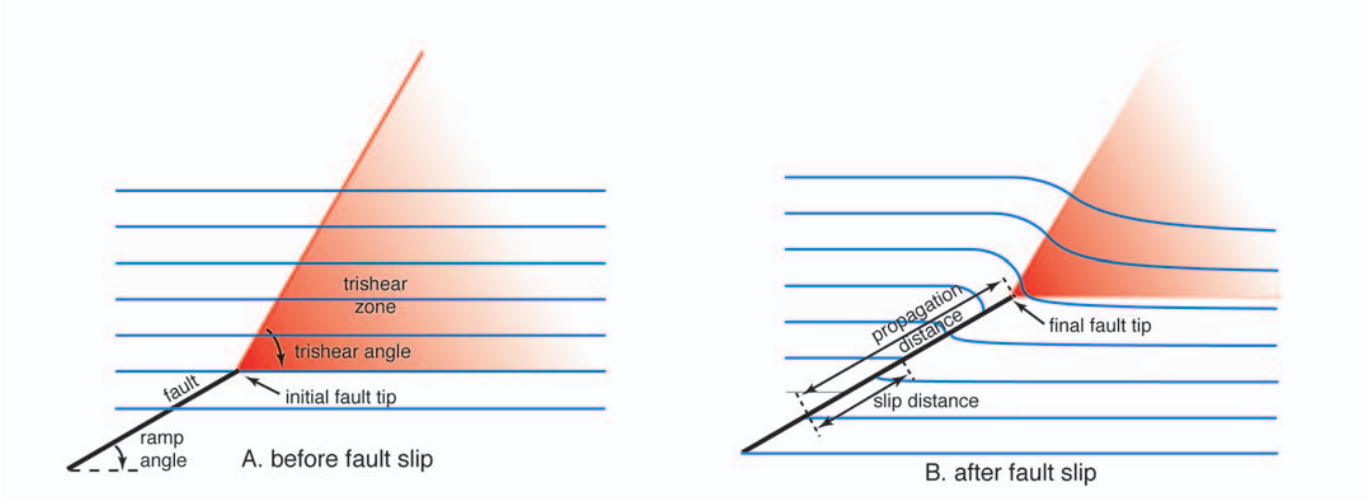

Figure 2. Schematic diagram of the trishear model (Erslev, 1991). Thick black line shows fault plane while red lines define the edges of the active trishear zone. Shading within the trishear zone reflects the intensity of deformation. Horizontal blue lines define stratigraphy. Note that strata below the initial fault tip remain unfolded after slip. Here deformation is distributed evenly across the trishear envelope (center concentration factor = 1).

based only on geometric modeling of the post-slip fold shape (Allmendinger and Shaw, 2000).

To date, the only model to explicitly consider the *p/s* ratio is the trishear model (Erslev, 1991; Hardy and Ford, 1997; Allmendinger, 1998). This model accommodates waning fault slip by folding within a triangular zone, the apex of which is pinned to the fault tip (Fig. 2A). Within this "trishear zone," particle velocities diminish along tie lines perpendicular to the fault, from a maximum in the hanging wall to zero in the footwall. The resulting fold geometry depends on seven variables, including the initial *x* and *y* locations of the fault tip, the fault dip (ramp angle), the total fault slip, the trishear angle, the *p/s* ratio, and the center concentration factor (*ccf*), which determines how folding is distributed within the trishear zone (Fig. 2B; Erslev, 1991; Erslev and Rogers, 1993; Hardy and Ford, 1997; Allmendinger, 1998). Fault dip and the location of the fault tip can often be determined from seismic data, and net slip may be determined from stratigraphic separation across the fault. Of the remaining three variables, *p/s* and *ccf* exert the most important control on fold shape (Allmendinger et al., 2003; E.A. Erslev, 2003, personal commun.). The *p/s* ratio determines how long a given packet of rock remains within the trishear envelope and consequently, how severely that packet is deformed. At low *p/s* values, packets spend a relatively long time within the trishear envelope and may accumulate very high strains. At higher *p/s* values, a given packet passes quickly through the trishear zone and therefore emerges relatively unstrained. Similarly, a high *ccf* will concentrate deformation in the center of the trishear zone, resulting in a local zone of highly strained rock.

For the purposes of this paper, the most important point is that all trishear folding occurs ahead of the initial location of the fault tip. The presence or absence of folding adjacent to the fault at a given horizon can thus be used as a clue to whether the fault began propagation from above or below that horizon. In the present case, it can be used to determine whether a given fault began propagation at or below the basement-cover contact.

LARAMIDE BASEMENT GEOMETRY

In the cases of the largest uplifts, such as the Colorado Front Range, erosion has removed the sedimentary cover and the uppermost basement, rendering it difficult or impossible to establish the geometry of the basement surface near the bounding faults. Outcrop exposures and seismic images of smaller uplifts, however, reveal a range of forms.

In some of these, the basement unconformity is clearly an undeformed, planar surface. Careful surveys of extensive exposures on Rattlesnake Mountain in northwest Wyoming and the Big Thompson anticline on the eastern edge of the Colorado Front Range both indicate that the basement surface is planar, and dike orientations show no sign of rotation at distances greater than 100 m from the fault (Stearns, 1978; Erslev and Rogers, 1993; Narr, 1993). Published seismic surveys reveal a number of other examples (Gries and Dyer, 1985; Stone, 1993a).

In other cases, surface exposures, seismic lines, and well-controlled cross sections clearly show that the basement surface is folded. (Here the term fold is used only to denote a curvature of the basement-cover contact, regardless of whether that curvature is achieved by flexural slip on subhorizontal foliation, distributed faulting, or some other means.) This folding occurs over a half wavelength of 100 m to 5 km (Table 1), where half wavelength is defined as the horizontal distance from flat-lying hanging wall to flat-lying footwall, or fault if the footwall is not imaged. Typical values are 500–1000 m. Within the fold, the basement surface may reach dips of 90° or even 75° overturned. At the other extreme, a few uplifts display basement surfaces that never exceed 10° of dip. Most fall in the range of 30°–60° (Table 1).

It is important to point out that there are several possible mechanisms for folding the basement surface, not all of them requiring an initial fault tip below that surface. First, damage incurred during fault slip might result in local curvature of the basement surface adjacent to the fault. In the cases described above, however, the relatively large horizontal scale of the

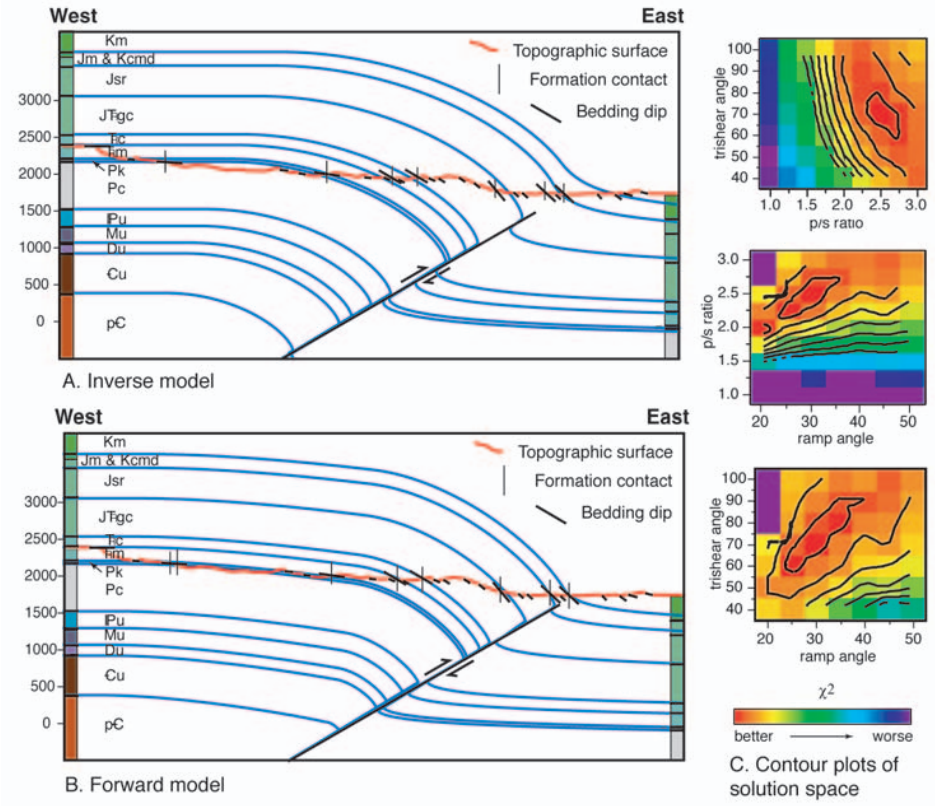

Figure 3. Inverse (A) and forward (B) models of the Waterpocket fold, based on mapping of a surface transect and regional thicknesses of undeformed strata. Elevations are in meters above sea level and cross sections are drawn without vertical exaggeration. Color bar on each side of cross sections shows ages of strata and vertical contact locations based on well logs and projection from the surface. **C:** Contour plots of errors in inverse modeling. Plots show two-dimensional slices through the three-dimensional matrix of error values produced by grid-searching for a best-fit over the specified ranges. Best fit is based on a chi-squared statistical analysis (Allmendinger, 1998). Note that all plots show well-defined regions of best fit.

deformation argues against this. Second, the basement surface may fold as a passive response to bends in the underlying fault (fault bend folding). Nearly all of the examples cited in Table 1 display some fault curvature, so this mechanism may well be responsible for some of the folding described above. However, the fault bends are generally quite small relative to the magnitude of basement folding. Finally, folding of the basement surface could be produced by buckling as a result of a "room problem" set up by horizontal shortening on a concave-upward fault (Coward, 1994). In such cases, however, folding is restricted entirely to the hanging wall, whereas many of the examples cited in Table 1 show folding of the basement surface in both hanging wall and footwall. For these reasons, it seems likely that fault-propagation folding created much of the observed basement curvature, a conclusion also reached by Stone (1993a) based on study of relations between fold shape and net fault slip.

TRISHEAR MODELING

Accepting that folding of the basement surface may reflect Laramide fault propagation from a point below that surface, a key question is how far below that surface did fault propagation begin. An estimate may be obtained from accurate trishear modeling of the structures in question. Current trishear modeling software allows an inverse grid search wherein each trishear model parameter is systematically and independently varied over a user-specified range while the program searches for a best-fit model. Although powerful, these programs are best applied to relatively simple structures and are not capable of handling some of the complexities commonly observed in the field, such as multiple fault strands, fault bends, or oblique slip.

One of the best-fitting models I have produced to date is for the Waterpocket monocline, which forms the steep eastern limb of the Circle Cliffs uplift in southern Utah (Fig. 1). Inverse modeling based on well logs and surficial exposures gives a reasonably good, though imperfect fit to the data (Fig. 3A). The principal problem is that the modeled fold wavelength is `too short, lacking the prolonged, gentle upper-limb dip observed in the field, and shallowing too quickly near the lower hinge. Forward modeling offers the possibility of improving the fit by allowing both spatial and temporal heterogeneity in trishear parameters. In the temporal case, the *p/s* ratio may be varied in accordance with the mechanical stratigraphy through which the fault propagates (Allmendinger, 1998). For the Waterpocket fold, initially rapid propagation (*p/s* = 6.0) through stiff basement rocks followed by slower propagation (*p/s* = 2.1) through less competent sedimentary rocks can produce the observed broad-wavelength fold with long, gently dipping upper and lower limbs and sharply steeper middle limb. Similar results may also be achieved through spatial heterogeneity, that is, by allowing folding to be concentrated toward the middle of the trishear zone, similar to deformation within a ductile shear zone (Erslev, 1991). The best-fit forward model is an excellent match for the data (Fig. 3B) and requires an initial fault tip 2.3 km below the basement-cover contact.

For other uplifts listed in Table 1, inverse modeling is limited by the complexity of observed fault geometries. Taking only those examples where both hanging wall and footwall are imaged and where >90% of the displacement is concentrated on a single fault leaves 15 possibilities for inversion. Of these, one is a seismic time section and is rejected for having too little true depth control. Three more have significantly curved faults and are also rejected. Of the remaining 11, only three have yielded reasonable inverse solutions. The eight failures are probably due to a combination of oblique slip and geometric complexities, including fault bends, problems in pinpointing the current location of the fault tip, and accurately migrating seismic data to show true depth.

Results for the three reasonable inverse models are quite varied. The bounding fault on Casper Mountain appears to have

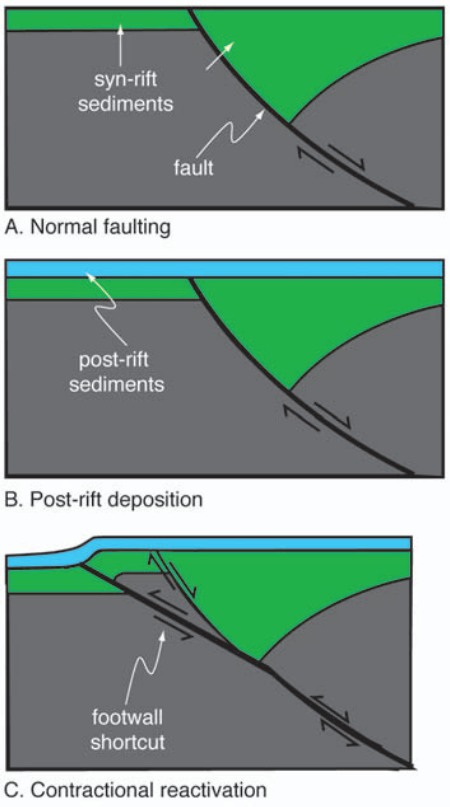

Figure 4. Schematic diagram of the creation of a listric normal fault (top) that is later reactivated in compression (bottom), creating a footwall shortcut. Pre-extensional rocks are shown in dark gray.

nucleated only 400–600 m below the basement surface, while the Island Park fault bounding the Uinta uplift appears to have begun propagation from a point 11 km below the basement surface. This is very close to the 12 km deep forethrust-backthrust junction shown by Stone (1993b) in a cross section of the Uintas. The fault underlying the Willow Creek anticline is in the middle, with an initial tip ~6 km below the basement surface (Fig. 3). Allmendinger's (1998) inversion of the Rangely anticline in Colorado shows an initial fault tip ~4 km below the basement surface, and an initial fault tip depth of 0.6 km below the basement surface for the San Rafael monocline in central Utah has also been found (personal observations; G.H. Davis, 2002, personal commun.).

The question arises as to whether any of these solutions are unique. Contour plots of the inverse modeling results (Fig. 3) suggest that the solution space is small and in controlled experiments with trishear inversions, Allmendinger et al. (2003) have found no local error minima in the inversion space that might be confused with the global minimum (Fig. 3C). That said, experience with the trishear modeling software shows that inverse models can almost always be refined and improved through forward modeling (Allmendinger et al., 2003) and the present models are probably no different. Furthermore, common sense suggests that with seven independently variable parameters, there are probably other solutions that satisfy the data. At present, the models described above are best-fits, but future efforts and continued development of trishear software may lead to further refinements.

DISCUSSION AND CONCLUSIONS

The evidence described above suggests that there is a wide spectrum of fault origins. Some uplifts, such as Rattlesnake Mountain and the Big Thompson anticline, show no evidence for deformation of the basement-cover contact and thus are probably bounded by ancient faults reactivated under Laramide compression. Many others (Table 1) do show deformation of the basement-cover contact. These appear to represent cases in which the bounding faults began propagation from deeper in the crust. Some of these, such as the Island Park fault, are probably entirely neoformed faults that branch off possibly older ones in the mid crust, forming as backthrusts in response to Laramide contraction. These end members are readily understood.

Several other faults, however, appear to have begun propagation from a few kilometers below the basement surface. The origin of these faults is less clear, as there is no obvious reason for a fault to begin propagation there. It is possible that they represent out-of-the-syncline thrusts (Brown, 1993), formed during the creation of larger folds. However, this requires that the folds described here be located in the proximal footwall of a larger fold, which is not true in general. It is also possible that these faults nucleated around point weaknesses within the basement, perhaps flaws or stress concentrators (Eisenstadt and DePaor, 1987; Allmendinger et al., 2003), though there is no clear reason to expect them at this crustal level.

Instead, I propose that they are footwall shortcuts (McClay, 1989; Coward, 1994), created by the compressional inversion of upward-steepening normal faults (Fig. 4). Almost all normal faults show some degree of concave-upward curvature (Coward, 1994). At the topographic surface, failure is often tensile or hybrid tensile-shear and the resulting fault dips are commonly near vertical. Dips decrease toward 60° at 3–4 km depth due to the change in failure mechanism from hybrid to shear fracturing (Walsh and Watterson, 1988). Proffet (1977) and Hamblin (1965) documented Basin and Range faults with dips that decreased at a rate of 0.5°–2° per 100 m of depth at near-surface levels. For crustal-scale faults, dips must decrease further toward 45° at ~10 km depth as the host rock rheology changes from brittle to plastic (Walsh and Watterson, 1988). Histograms showing numbers of seismically active normal faults versus fault dip typically exhibit strong peaks at 45° (Thatcher and Hill, 1991; Collettini and Sibson, 2001). Finally, if the fault is detached at some deeper level, then it must eventually bend toward horizontal. Seismic activity has been documented on normal faults with dips as low as 30° (Collettini and Sibson, 2001).

The structural level of the current basement surface with respect to Precambrian normal faults is uncertain. The Grand and Salt River Canyons expose Precambrian normal faults dipping 60°–85° at the basement-cover contact (Davis et al., 1981; Huntoon, 1993), which suggests a shallow structural level. In the Grand Canyon, the hanging walls are composed of syn-rift sedimentary rocks (Timmons et al., 2001), also consistent with ideas suggesting that the current basement surface may not have been far below the syn-extensional topographic surface. On the other hand, Ar-Ar evidence suggests that >6 km of rock was eroded between widespread extensional faulting at 800 and 1100 Ma and Cambrian deposition (Heizler et al., 2000), which would indicate that current exposures represent deeper levels of the Precambrian normal fault systems (Marshak et al., 2000) that were reactivated in the Laramide. In either case, however, the exposed faults are steep where they intersect the basement unconformity.

Under horizontal compression, it is easiest to reactivate faults dipping 25°–40° (Byerlee, 1978; Ranalli, 2000). At higher dips, it is often easier to create a new, lower-angle fault than to reactivate the old, steep one. Dip catalogs of seismically

TABLE 1. EXAMPLES OF FOLDED BASEMENT-COVER CONTACT

North flank, Uinta Mountains	4	2.3	115	85	cross section[1, 2]	Gries, 1983
Anticline in North McCallum field	5	0.6	160	10	seismic line[4]	Lange and Wellborn, 1985
Anticline in Battleship field	6	0.3	165	10	seismic line[4]	Lange and Wellborn, 1985
Rangely anticline	7	0.7	80	75	cross section[1, 2]	Mitra and Mount, 1998
Twin Mountain anticline	8	0.1	70	85*	cross section[5]	Schmidt et al., 1993
Big Thompson anticline	9	0.5	75	90	cross section[5, 7]	Narr and Suppe, 1994
Willow Creek anticline	10	1.0	100	80	cross section[1]	Narr and Suppe, 1994
Laramie basin	11	0.8	145	21	seismic line[3]	Stone, 1993a
Oregon Basin thrust	12	4.0	130	50	seismic line[3]	Stone, 1993a
Pitchfork anticline	13	0.3	115	35	cross section[1, 2]	Stone, 1993a
Elk Basin anticline	14	0.4	100	50	cross section[1, 2]	Stone, 1993a
Maverick Springs anticline	15	4.0	60	40	cross section[2, 5]	Stone, 1993a
Small anticline on Casper Mountain	16	0.1	105	90	cross section[6]	Narr, 1993
Five Springs thrust, Bighorn Mountains	17	0.7	85	65	cross section[6]	Narr and Suppe, 1994; Wise and Obi, 1992
Rawlins uplift	18	>1.3	70	75*	cross section	Gries, 1983
Granite Mountains	19	2.5	150	34	cross section	Gries, 1983
LaPrele anticline	20	0.6	70	90	cross section[5]	Schmidt et al., 1993
Sheephead Mountain anticline	21	0.1	60	75*	cross section[5]	Chase et al., 1993
Madden anticline	22	5.0	160	10	cross section[1, 2]	Ray and Keefer, 1985
London Hills anticline	23	0.5	110	90	cross section[5]	Chase et al., 1993

Note: Asterisk indicates overturned; 1—seismic control; 2—well control; 3—time section; 4—depth section; 5—down-plunge projection; 6—surface control only; 7—gravity control.

active reverse faults typically show a cut off at 60° (Sibson and Xie, 1998; Collettini and Sibson, 2001). Upward-steepening normal faults are thus susceptible to pure reverse-sense reactivation only where they dip less than ~60°, i.e., in their lower extents, at depths >3–4 km beneath the contemporary topographic surface. The upper, steep portion is difficult or impossible to reactivate in pure reverse motion which often leads to the creation of one or more "footwall shortcuts," i.e., splays that branch off the old fault and form new, lower angle routes to the surface, bypassing the steep segment of the original fault (Fig. 4; McClay, 1989; Coward, 1994). These may be unequivocally identified if the abandoned portion of the fault retains normal-sense offset whereas the new splay shows reverse offset. The hanging wall may also include a half graben of older sedimentary rocks and/or an ancient shear zone of steeper dip than the uplift-bounding fault.

In the spirit of Davis (1926) and Wise (1963), this is both a hypothesis to be tested and an attractive idea as it offers a means to unify the end-member interpretations. The scatter in Laramide fault strikes may well reflect tectonic inheritance. Marshak et al. (2000) presented a compelling comparison of the large-scale Laramide fault geometry to that of rift systems exposed in the southern Rockies, and Timmons et al. (2001) documented multiple episodes of Precambrian extensional faulting. At the same time, the fact remains that relatively few Laramide faults show unequivocal evidence of reactivation. This work suggests that ancient faults can be reactivated at depth but form new paths to the surface. The large-scale geometry of the orogen may thus be controlled by ancient structures but the surficially exposed segments of the faults need not be ancient themselves.

In the broader picture, this work suggests that there is an entire spectrum of faults ranging from 100% neoformed to 100% reactivated. Many, perhaps even a majority, of intracontinental faults lie between these end members. Under compressive stress, weak sections of existing faults may localize the initial failure. Bends or other strength heterogeneities in those faults, however, may necessitate the growth of new, more favorably oriented segments if slip continues. Perhaps the resulting fault, such as might typify the Laramide or any other zone of intracratonic shortening, is thus a hybrid of linked ancient and neoformed segments and exhibits characteristics of both.

ACKNOWLEDGMENTS

The manuscript has benefited from discussion with David Ferrill, Clem Chase, Ofori Pearson, and George Davis, and review by Don Wise, Jon Spencer, Gautam Mitra, Eric Erslev, John Suppe, and Karl Karlstrom. Special thanks go to Eric Erslev who pointed out ambiguities in the trishear approach to Laramide structures. Trishear software was generously provided by Rick Allmendinger and Nestor Cardozo. Funding was provided by National Science Foundation grant EAR-0001222 (awarded to George Davis). My thanks to them all.

REFERENCES CITED

Allmendinger, R.W., 1998, Inverse and forward numerical modeling of trishear fault-propagation folds: Tectonics, v. 17, p. 640–656.

Allmendinger, R.W., and Shaw, J.H., 2000, Estimation of fault propagation distance from fold shape: Implications for earthquake hazard assessment: Geology, v. 28, p. 1099–1102.

Allmendinger, R.W., Zapata, T., Manceda, R., and Dzelalija, F., 2003, Trishear kinematic modeling of structures with examples from the Neuquen Basin, Argentina: American Association of Petroleum Geologists (in press).

Axen, G.J., Selverstone, J., Byrne, T., and Fletcher, J.M., 1998, If the strong crust leads will the weak crust follow?: GSA Today, v. 8, no. 12, p. 1–8.

Brown, W.G., 1993, Structural style of Laramide basement-cored uplifts and associated folds, *in* Snoke, A.W., et al., eds., Geology of Wyoming: Geological Survey of Wyoming Memoir No. 5, p. 312–371.

Byerlee, J.D., 1978, Friction of rocks: Pure and Applied Geophysics, v. 116, p. 615–626.

Chase, R.B., Schmidt, C.J., and Genovese, P.W., 1993, Influence of Precambrian rock compositions and fabrics on the development of Rocky Mountain foreland folds, *in* Schmidt, C.J., et al., eds., Laramide basement deformation in the Rocky Mountain foreland of the western United States: Boulder, Colorado, Geological Society of America Special Paper 280, p. 45–72.

Collettini, C., and Sibson, R.H., 2001, Normal faults, normal friction?: Geology, v. 29, p. 927–930.

Coward, M., 1994, Inversion tectonics, *in* Hancock, P., ed., Continental deformation: New York, Pergamon Press, p. 289–304.

Davis, G.H., Showalter, S.R., Benson, G.S., and McCalmont, L.S., 1981, Guide to the geology of the Salt River Canyon region, Arizona: Arizona Geological Society Digest, v. 13, p. 49–97.

Davis, W.M., 1926, The value of the outrageous geological hypothesis: Science, v. 63, p. 463–468.

Eisenstadt, G., and DePaor, D., 1987, Alternative model of thrust-fault propagation: Geology, v. 15, p. 630–633.

Erslev, E.A., 1991, Trishear fault-propagation folding: Geology, v. 19, p. 617–620.

Erslev, E.A., 1993, Thrusts, back-thrusts, and detachment of Rocky Mountain foreland arches, *in* Schmidt, C.J., et al., eds., Laramide basement deformation in the Rocky Mountain foreland of the western United States: Boulder, Colorado, Geological Society of America Special Paper 280: p. 339–359.

Erslev, E.A., and Rogers, J.L., 1993, Basement-cover geometry of Laramide fault-propagation folds, *in* Schmidt, C.J., et al., eds., Laramide basement deformation in the Rocky Mountain foreland of the western United States: Boulder, Colorado, Geological Society of America Special Paper 280, p. 125–146.

Gries, R., 1983, North-south compression of Rocky Mountain foreland structures, *in* Lowell, J.D., ed., Rocky Mountain foreland basins and uplifts: Denver, Rocky Mountain Association of Geologists, p. 9–32.

Gries, R.R., and Dyer, R.C., 1985, Seismic exploration of the Rocky Mountain region: Denver, Rocky Mountain Association of Geologists and Denver Geophysical Society, p. 300.

Hamblin, W.K., 1965, Origin of "reverse drag" on the downthrown side of normal faults: Geological Society of America Bulletin, v. 76, p. 1145–1164.

Hamilton, W.B., 1988, Laramide crustal shortening, *in* Schmidt, C.J., and Perry, W.J., Jr., eds., Interaction of the Rocky Mountain foreland and the Cordilleran thrust belt: Boulder, Colorado, Geological Society of America Memoir 171, p. 27–40.

Hardy, S., and Ford, M., 1997, Numerical modeling of trishear fault propagation folding: Tectonics, v. 16, p. 841–854.

Heizler, M.T., Timmons, J.M., and Karlstrom, K.E., 2000, Ancestry of Ancestral Rocky Mountain faults: Geological Society of America Abstracts with Programs, v. 32, no. 7, p. A-465.

Hintze, L.F., 1980, Geologic map of Utah: Salt Lake City, Utah Geological and Mineral Survey.

Holdsworth, J.A., Buick, R.E., and Hand, M., 2001, Continental reactivation and reworking: London, Geological Society of London Special Publication 184, 408 p.

Huntoon, P.W., 1993, Influence of inherited Precambrian basement structure on the localization and form of Laramide monoclines, Grand Canyon, Arizona, *in* Schmidt, C.J., et al., eds., Laramide basement deformation in the Rocky Mountain foreland of the western United States: Boulder, Colorado, Geological Society of America Special Paper 280, p. 243–256.

Jackson, J., 2002, Strength of the continental lithosphere: Time to abandon the jelly sandwich?: GSA Today, v. 12, no. 9, p. 4–10.

King, P.B., 1969, Tectonic map of North America: Washington, U.S. Geological Survey.

Lange, J.K., and Wellborn, R.E., 1985, Seismic profile: North Park Basin, *in* Gries, R.R., and Dyer, R.C., eds., Seismic exploration of the Rocky Mountain region: Denver, Rocky Mountain Association of Geologists and Denver Geological Society, p. 239–245.

Love, J.D., and Christiansen, A.C., 1985, Geologic map of Wyoming: Reston, Virginia, U.S. Geological Survey.

Marshak, S., Karlstrom, K., and Timmons, J.M., 2000, Inversion of Proterozoic extensional faults: An explanation for the pattern of Laramide and Ancestral Rockies intracratonic deformation, United States: Geology, v. 28, p. 735–738.

McClay, K.R., 1989, Analogue models of inversion tectonics, *in* Cooper, M.A., and Williams, G.D., eds., Inversion tectonics: London, Geological Society of London Special Publication 44, p. 41–59.

Mitra, G., and Frost, B.R., 1981, Mechanisms of deformation within Laramide and Precambrian deformation zones in basement rocks of the Wind River Mountains: University of Wyoming Contributions to Geology, v. 19, p. 161–173.

Mitra, S., and Mount, V.S., 1998, Foreland basement-involved structures: American Association of Petroleum Geologists Bulletin, v. 82, p. 70–109.

Narr, W., 1993, Deformation of basement in basement-involved compressive structures, *in* Schmidt, C.J., et al., eds., Laramide basement deformation in the Rocky Mountain foreland of the western United States: Boulder, Colorado, Geological Society of America Special Paper 280, p. 107–124.

Narr, W., and Suppe, J., 1994, Kinematics of basement-involved compressive structures: American Journal of Science, v. 294, p. 802–860.

Proffett, J.M., Jr., 1977, Cenozoic geology of the Yerington District, Nevada, and implications for the nature and origin of Basin and Range faulting: Geological Society of America Bulletin, v. 88, p. 247–266.

Ranalli, G., 2000, Rheology of the crust and its role in tectonic reactivation: Journal of Geodynamics, v. 30, p. 3–15.

Ray, R.R., and Keefer, W.R., 1985, Wind River Basin, central Wyoming, *in* Gries, R.R., and Dyer, R.C., eds., Seismic exploration of the Rocky Mountain Region: Denver, Rocky Mountain Association of Geologists and Denver Geological Society, p. 201–212.

Schmidt, C.J., and Garihan, J.M., 1983, Laramide tectonic development of the Rocky Mountain foreland of southwestern Montana, *in* Lowell, J.D., ed., Rocky Mountain foreland basins and uplifts: Denver, Rocky Mountain Association of Geologists, p. 271–294.

Schmidt, C.J., Genovese, P.W., and Chase, R.B., 1993, Role of basement fabric and cover-rock lithology on the geometry and kinematics of twelve folds in the Rocky Mountain foreland, *in* Schmidt, C.J., et al., eds., Laramide basement deformation in the Rocky Mountain foreland of the western United States: Boulder, Colorado, Geological Society of America Special Paper 280, p. 1–44.

Sibson, R.H., 1977, Fault rocks and fault mechanisms: Journal of the Geological Society of London, v. 133, p. 191–213.

Sibson, R.H., and Xie, G.Y., 1998, Dip range for intracontinental reverse fault ruptures: Truth not stranger than friction?: Bulletin of the Seismological Society of America, v. 88, p. 1014–1022.

Stearns, D.W., 1978, Faulting and forced folding in the Rocky Mountain foreland, *in* Matthews, V.I., ed., Laramide folding associated with basement block faulting in the western United States: Boulder, Colorado, Geological Society of America Memoir 151, p. 1–37.

Stone, D.S., 1993a, Basement-involved thrust-generated folds as seismically imaged in the subsurface of the central Rocky Mountain foreland, *in* Schmidt, C.J., et al., eds., Laramide basement deformation in the Rocky Mountain foreland of the western United States: Boulder, Colorado, Geological Society of America Special Paper 280, p. 271–312.

Stone, D.S., 1993b, Tectonic evolution of the Uinta mountains: Palinspastic restoration of a structural cross-section along longitude 109º15′, Utah: Salt Lake City, Utah Geological Survey, 19 p.

Suppe, J., and Medwedeff, D.A., 1990, Geometry and kinematics of fault-propagation folding: Ecolgae Geologicae Helvetiae, v. 83, p. 409–454.

Thatcher, W., and Hill, D.P., 1991, Fault orientations in extensional and conjugate strike-slip environments and their implications: Geology, v. 19, p. 1116–1120.

Timmons, J.M., Karlstrom, K.E., Dehler, C.M., Geissman, J.W., and Heizler, M.T., 2001, Proterozoic multistage (ca. 1.1 and 0.8 Ga) extension recorded in the Grand Canyon Supergroup and establishment of northwest- and north-trending grains in the southwestern United States: Geological Society of America Bulletin, v. 113, p. 163–180.

Tweto, O., 1979, Geologic map of Colorado: Denver, Colorado, U.S. Geological Survey.

Walcott, C.D., 1890, Study of a line of displacement in the Grand Canyon of the Colorado, in northern Arizona: Geological Society of America Bulletin, v. 1, p. 49–64.

Walsh, J.J., and Watterson, J., 1988, Dips of normal faults in British Coal Measures and other sedimentary sequences: Journal of the Geological Society of London, v. 145, p. 859–873.

Wise, D.U., 1963, An outrageous hypothesis for the tectonic pattern of the North American Cordillera: Geological Society of America Bulletin, v. 74, p. 357–362.

Wise, D.U., and Obi, C.M., 1992, Laramide basement deformation in an evolving stress field, Bighorn mountain front, Five Springs area, Wyoming: American Association of Petroleum Geologists Bulletin, v. 76, p. 1586–1600.

Yin, A., 1994, Mechanics of monoclinal systems in the Colorado Plateau during the Laramide orogeny: Journal of Geophysical Research, v. 99, p. 22,043–22,058.

Manuscript submitted November 14, 2002; accepted January 15, 2003. ❖